

## Supplementary Materials for

### Highly bioactive zeolitic imidazolate framework-8–capped nanotherapeutics for efficient reversal of reperfusion-induced injury in ischemic stroke

Lizhen He, Guanning Huang, Hongxing Liu, Chengcheng Sang, Xinxin Liu, Tianfeng Chen\*

\*Corresponding author. Email: [tcchentf@jnu.edu.cn](mailto:tcchentf@jnu.edu.cn)

Published 18 March 2020, *Sci. Adv.* **6**, eaay9751 (2020)

DOI: 10.1126/sciadv.aay9751

#### This PDF file includes:

- Fig. S1. Characterization of the synthetic nanomaterials.
- Fig. S2. Examination of free radical scavenging activity of the nanotherapeutics.
- Fig. S3. N<sub>2</sub> adsorption-desorption isotherm and pore property analysis.
- Fig. S4. CeO<sub>2</sub>@ZIF-8 inhibits cell apoptosis and ROS overproduction induced by t-BOOH.
- Fig. S5. Change in cell microstructure and mice body weight.
- Fig. S6. Brain protection effects of CeO<sub>2</sub>@ZIF-8 in C57 MCAO mice.
- Fig. S7. Fluorescence imaging and biodistribution analysis of CeO<sub>2</sub>@ZIF-8 in vivo.
- Fig. S8. H&E staining of the heart, liver, spleen, lung, and kidney after treatment with CeO<sub>2</sub>@ZIF-8 for 3 days in MCAO mice model.
- Fig. S9. Toxicity evaluation of CeO<sub>2</sub>@ZIF-8 in vivo.
- Table S1. Pharmacokinetic parameters of CeO<sub>2</sub> nanopolyhedra and CeO<sub>2</sub>@ZIF-8 composite nanomaterials.

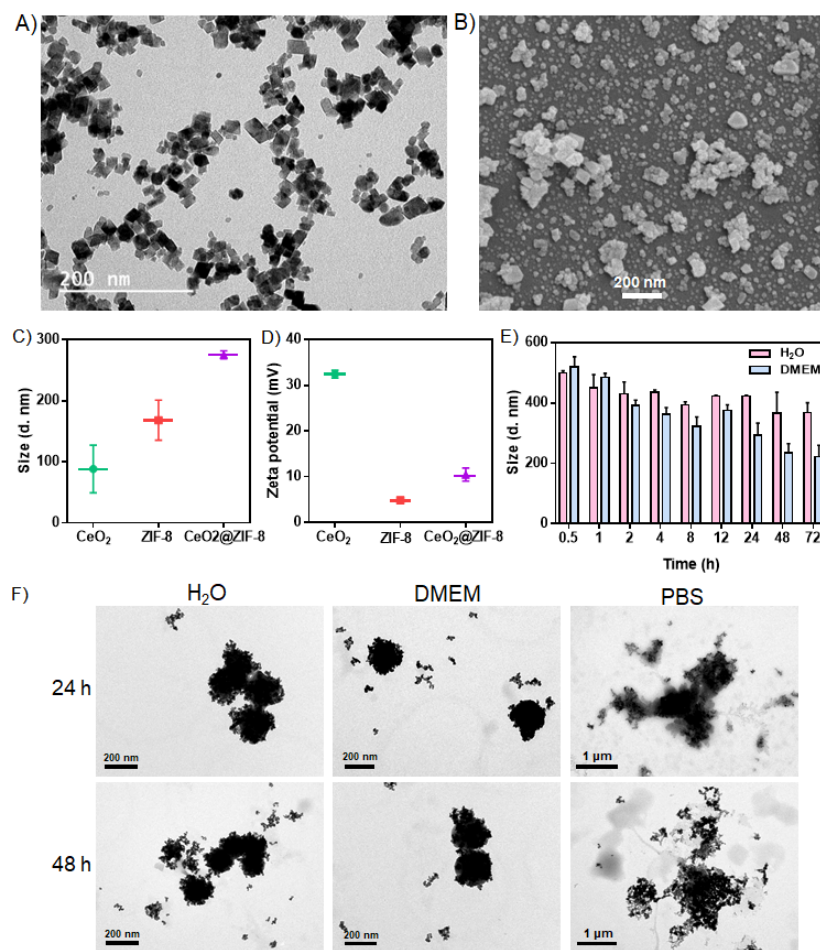


**Fig. S1. Characterization of the synthetic nanomaterials.** TEM image (A) and SEM image (B) of CeO<sub>2</sub> polyhedron. The size distribution (C) and zeta potential (D) of CeO<sub>2</sub>, ZIF-8 and CeO<sub>2</sub>@ZIF-8 nanomaterials. (E) Stability of CeO<sub>2</sub>@ZIF-8 in aqueous solution and DMEM medium. (F) TEM images of CeO<sub>2</sub>@ZIF-8 in H<sub>2</sub>O, DMEM (with 10% FBS), PBS (pH 7.4) after shaking for 24 h and 48 h.

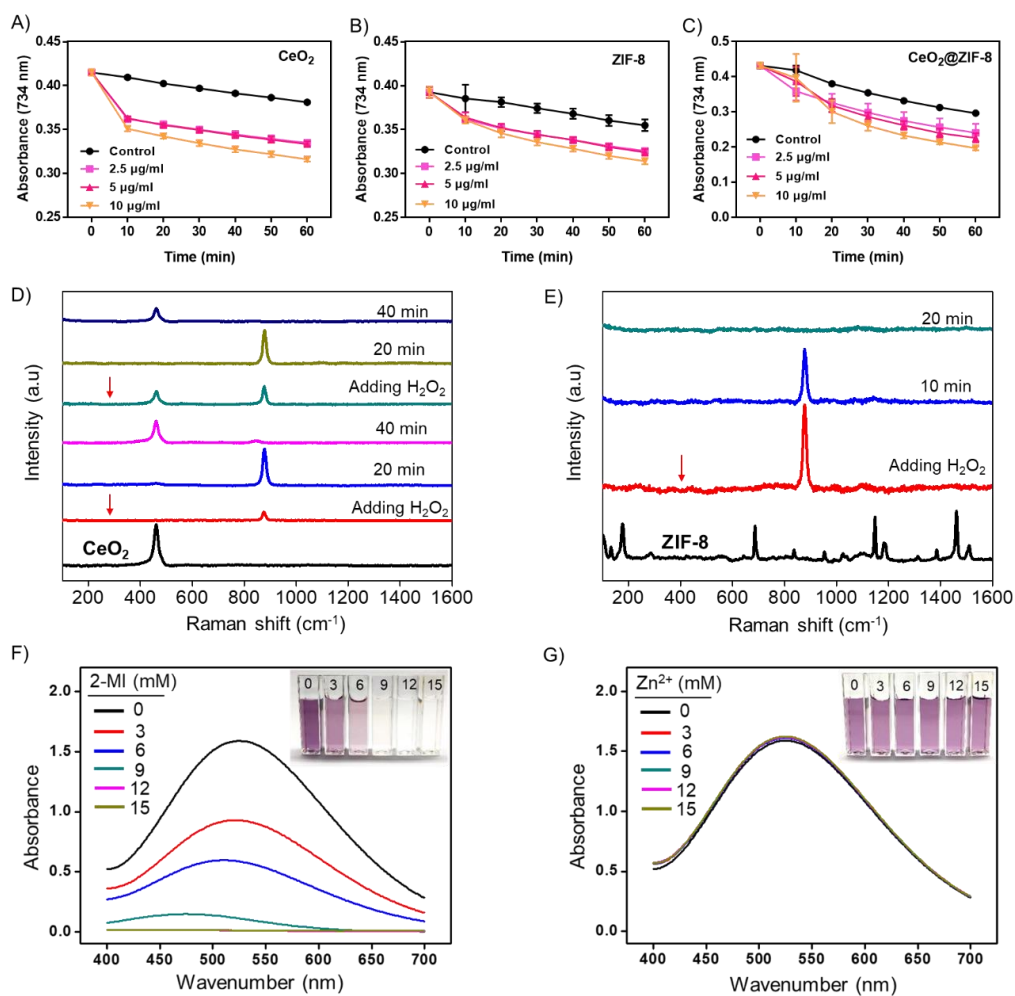


**Fig. S2. Examination of free radical scavenging activity of the nanotherapeutics.** Examination of antioxidant activities of  $\text{CeO}_2$  (A), ZIF-8 (B) and  $\text{CeO}_2@ZIF-8$  (C) by ABTS assay. Raman spectra of  $\text{CeO}_2$  (D) and ZIF-8 (E) after reaction with  $\text{H}_2\text{O}_2$  at various time points. The  $\cdot\text{OH}$  scavenging ability of 2-methylimidazolate (2-MI) (F) and  $\text{Zn}(\text{NO}_3)_2 \cdot 6\text{H}_2\text{O}$  ( $\text{Zn}^{2+}$ ) (G) at indicated concentrations as examined by UV-Vis spectroscopic analysis of salicylic acid (SA) interaction with  $\cdot\text{OH}$  generated by Fenton reaction with  $\text{Fe}^{2+}/\text{H}_2\text{O}_2$  system for 10 min.

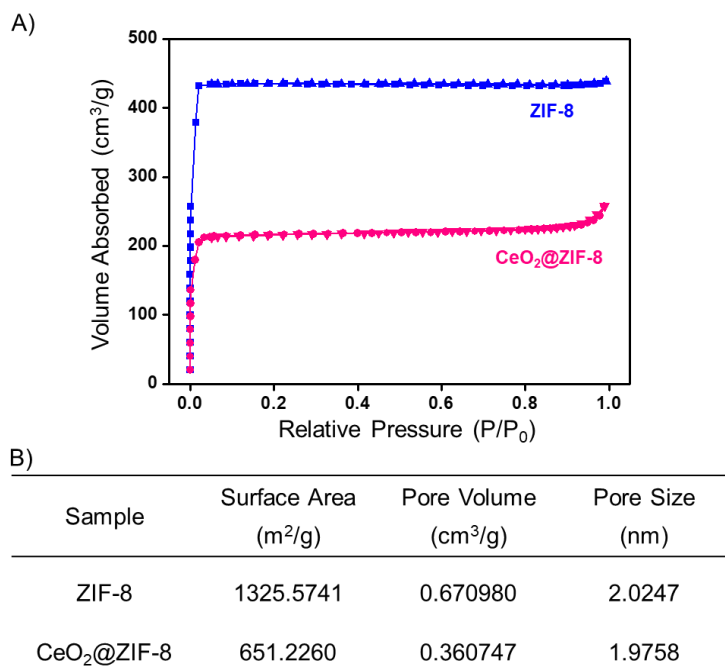


**Fig. S3. N<sub>2</sub> adsorption-desorption isotherm and pore property analysis.** (A) N<sub>2</sub> adsorption-desorption isotherm for ZIF-8 and CeO<sub>2</sub>@ZIF-8 NPs. (B) The surface area, pore volume and pore size of ZIF-8 and CeO<sub>2</sub>@ZIF-8.

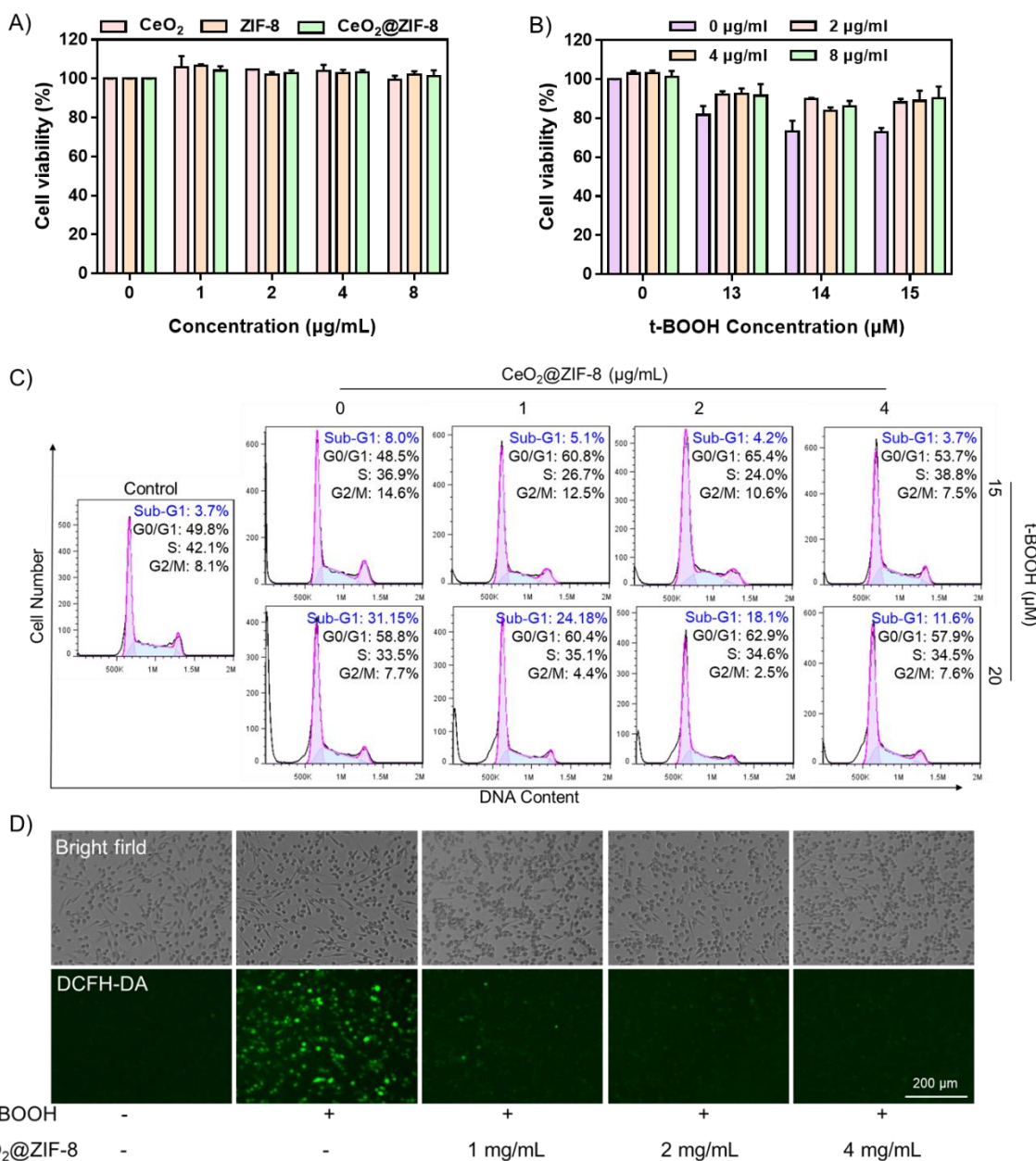


**Fig. S4. CeO<sub>2</sub>@ZIF-8 inhibits cell apoptosis and ROS overproduction induced by t-BOOH.** (A) The cell viability of PC-12 cells treated with different concentrations of CeO<sub>2</sub>, ZIF-8 and CeO<sub>2</sub>@ZIF-8 NPs for 48 h. (B) CeO<sub>2</sub>@ZIF-8 attenuated t-BOOH-induced cytotoxicity in PC-12 cells damaged with different concentration of t-BOOH. (C) CeO<sub>2</sub>@ZIF-8 reversed t-BOOH-induced apoptosis in PC-12 cells for 48 h. Cell cycle distribution was analysed by flow cytometric. (D) CeO<sub>2</sub>@ZIF-8 blocks t-BOOH (15 µM)-induced ROS generation in PC-12 cells for 2 h.

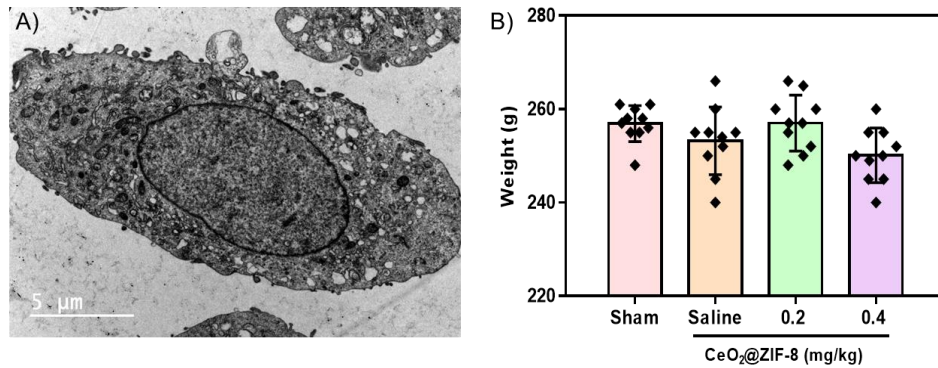


**Fig. S5. Change in cell microstructure and mice body weight.** (A) TEM image of PC-12 cells in control group. (B) The body weight of MCAO mice with different treatment (3 days).

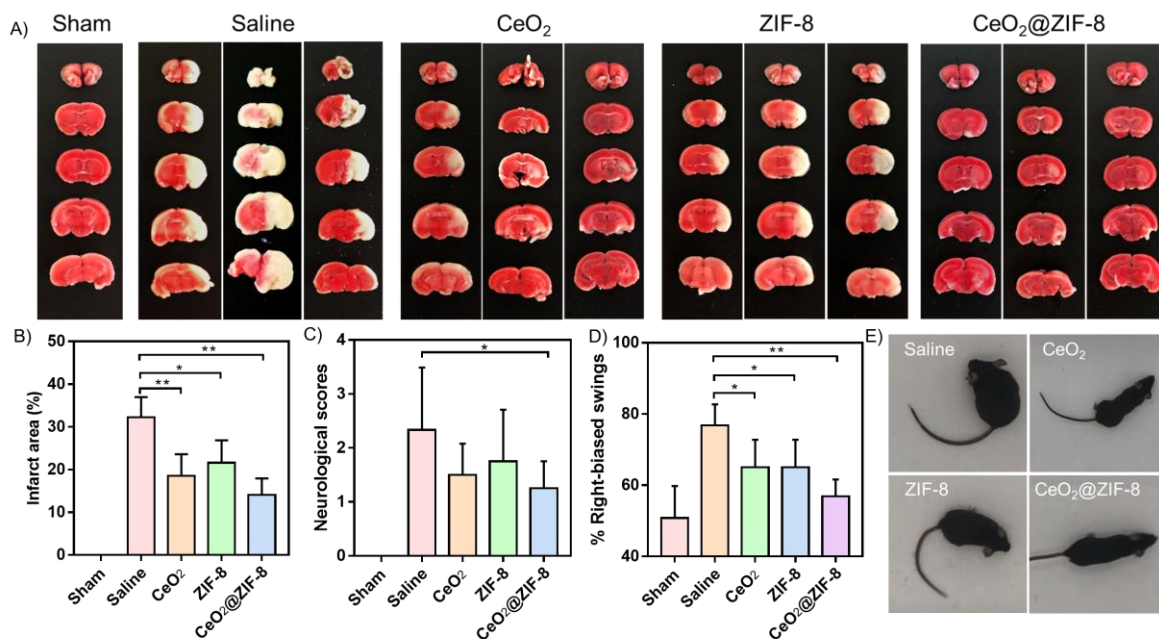


**Fig. S6. Brain protection effects of CeO<sub>2</sub>@ZIF-8 in C57 MCAO mice.** (A) Representative images of TTC-stained brain slices after treatment with CeO<sub>2</sub>, ZIF-8 and CeO<sub>2</sub>@ZIF-8 at 0.4 mg/kg for 3 days in MCAO mice model (n = 4). (B) Corresponding infarct areas of different groups analyzed by Image J (n = 4). (C) Neurological scores of MCAO mice after treatment with CeO<sub>2</sub>@ZIF-8 for 3 days (n = 4). (D) Changes in function and behavior of MCAO mice after different treatments as evaluated by elevated body swing test (EBST). (E) Representative images of behavioral recovery of MCAO mice after different treatments. (Photo credit: Guanning Huang, Jinan University).

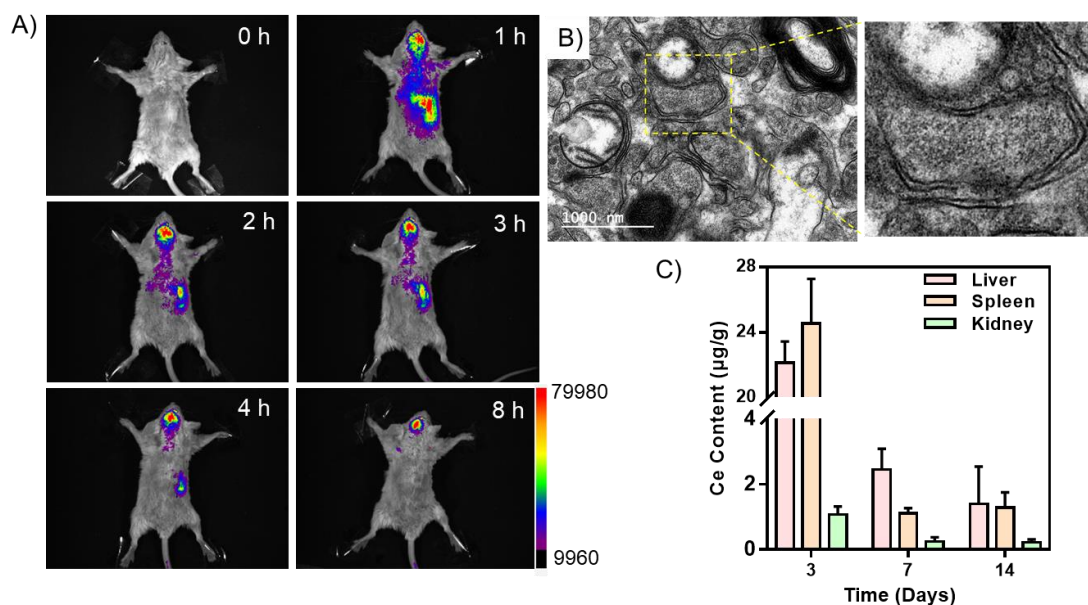


**Fig. S7. Fluorescence imaging and biodistribution analysis of CeO<sub>2</sub>@ZIF-8 in vivo.** (A) Fluorescence imaging of accumulation of ICG-labelled CeO<sub>2</sub>@ZIF-8 (0.4 mg/kg) in MCAO mice model at different time points. (B) TEM image of brain tissue of MCAO mice with saline injection only. (C) Biodistribution of Ce in the mice main organs (including liver, spleen and kidney) after intravenous injection with CeO<sub>2</sub>@ZIF-8 (0.4 mg/kg) for different periods of time (n = 5).

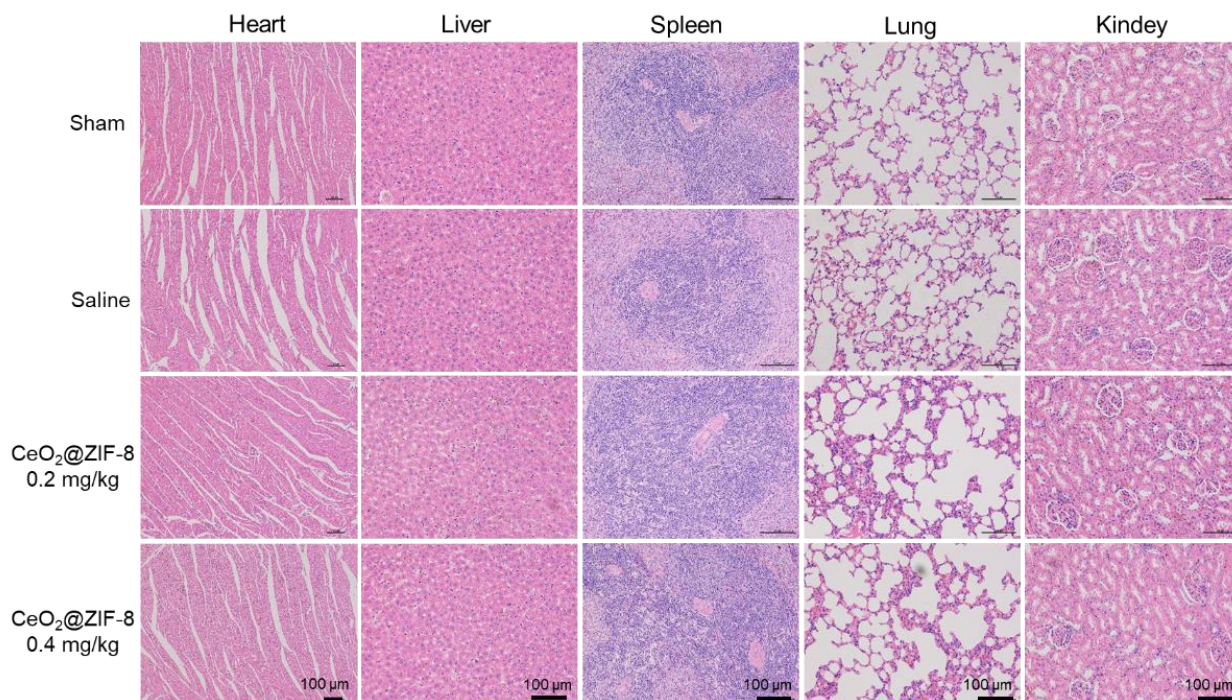


**Fig. S8. H&E staining of the heart, liver, spleen, lung, and kidney after treatment with CeO<sub>2</sub>@ZIF-8 for 3 days in MCAO mice model.**

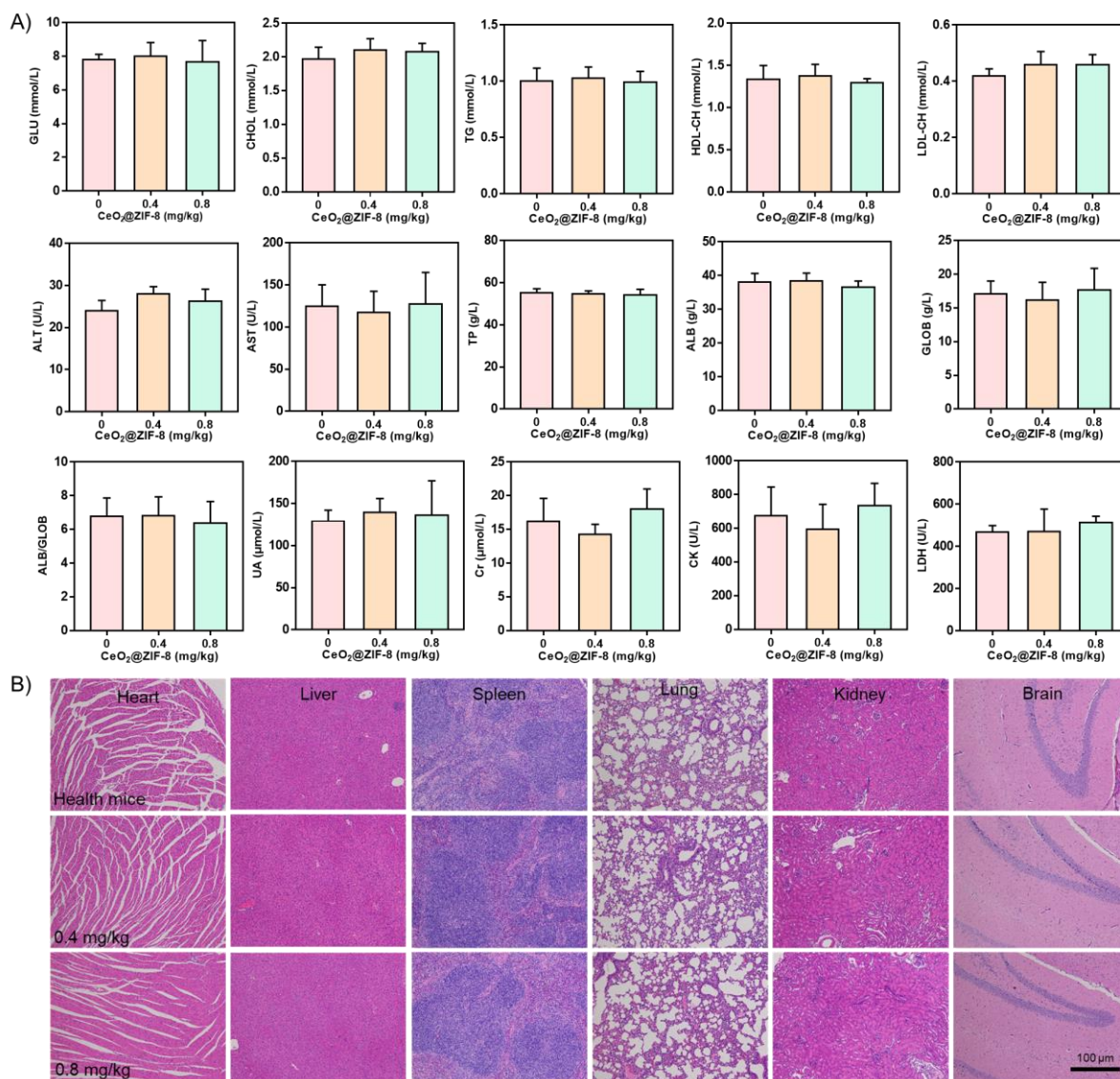


**Fig. S9. Toxicity evaluation of CeO<sub>2</sub>@ZIF-8 in vivo.** (A) Haematological analysis of blood glucose, blood fat, the function of liver, kidney and heart in CeO<sub>2</sub>@ZIF-8-treated mice for 14 days (n=6). (B) H&E staining of the heart, liver, spleen, lung, kidney and brain tissue after treatment with CeO<sub>2</sub>@ZIF-8 for 14 days (n=6).



**Table S1. Pharmacokinetic parameters of CeO<sub>2</sub> nanopolyhedra and CeO<sub>2</sub>@ZIF-8 composite nanomaterials.**

Parameter	Unit	CeO <sub>2</sub> NPs	CeO <sub>2</sub> @ZIF-8 NPs
		Value	Value
k10	1/h	0.0623	0.0112
k12	1/h	1.8406	0.1078
k21	1/h	0.3210	0.2409
t1/2Alpha	h	0.3129	1.9667
t1/2Beta	h	76.6648	89.7881
C0	µg/ml	2.6253	0.7258
V	(µg)/(µg/ml)	38.0903	137.7729
CL	(µg)/(µg/ml)/h	2.3758	1.5554
V2	(µg)/(µg/ml)	218.3612	61.6702
CL2	(µg)/(µg/ml)/h	70.1104	14.8615
AUC 0-t	µg/ml*h	20.6692	27.7958
AUC 0-inf	µg/ml*h	42.0901	64.2914
AUMC	µg/ml*h <sup>2</sup>	4543.2473	8243.7547
MRT	h	107.9408	128.2248
Vss	µg/(µg/ml)	256.4516	199.4431